Atmospheric Environment 358 (2025) 121308

Contents lists available at ScienceDirect

Atmospheric Environment

journal homepage: www.elsevier.com/locate/atmosenv

Investigating the long-range dispersion of atmospheric microplastics in the free atmosphere with a numerical model

Matteo M. Musso [a], Silvia Trini Castelli [b,*]

[a] Department of Physics, University of Torino, Torino, Italy
[b] Institute of Atmospheric Sciences and Climate, National Research Council, Torino, Italy

GRAPHICAL ABSTRACT

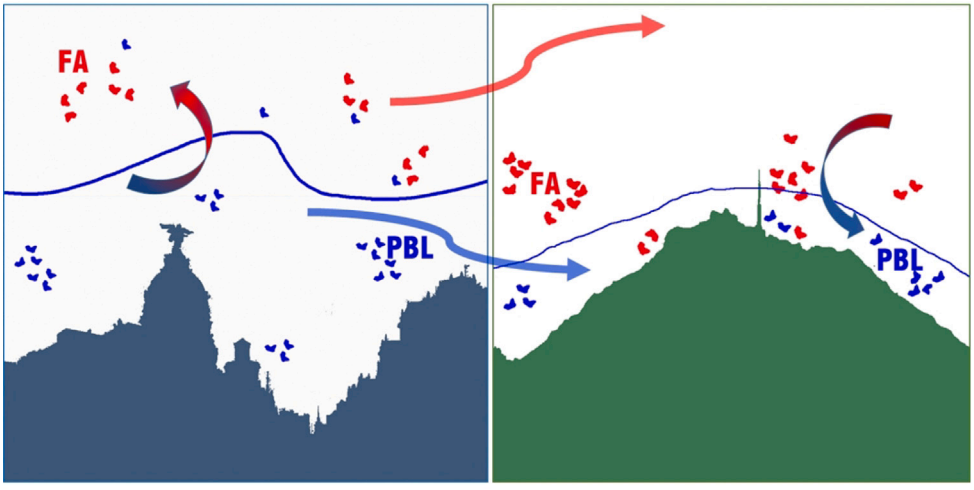

Representation of the exchange between microplastics in the Planetary Boundary Layer (blue colour, PBL) and microplastics in the Free Atmosphere (red colour, FA), over Madrid city (left panel) and over Pic Du Midi mountain (right panel), and of the transport from sources (cities) to remote places (mountains).

HIGHLIGHTS

- Long-range transport has the main role for microplastic pollution in free atmosphere.
- Microplastics from urban sites enter the free atmosphere mostly far from the release.
- The sea is confirmed to be a potential source of microplastics in the atmosphere.

ARTICLE INFO

Keywords:
Atmospheric microplastics
Backward dispersion

ABSTRACT

In recent studies available in literature, long-range transport was suggested to play a main role in the motion of microplastics in the free atmosphere, whereas emission sources are located in the planetary boundary layer. In this framework, the Lagrangian particle dispersion model MILORD was used both in forward and

* Corresponding author.
E-mail address: s.trinicastelli@isac.cnr.it (S. Trini Castelli).

https://doi.org/10.1016/j.atmosenv.2025.121308
Received 24 July 2024; Received in revised form 8 May 2025; Accepted 17 May 2025
Available online 4 June 2025

Long-range transport
Free atmosphere
MILORD Lagrangian model
Numerical simulation

in backward modes to investigate the potential effectiveness of the transport and exchange of microplastics between the boundary layer and the free atmosphere. Two pioneering case studies from the literature were considered. The first where microplastics were detected in the free atmosphere above Madrid region, the second where microplastics were collected in the air at the top-mountain site of Pic Du Midi in the French Pyrenees. The simulations showed that the long-range transport plays the main role in determining the presence of microplastics in the free atmosphere above Madrid, while the emissions from the city affect mostly the air in the boundary layer, at regional scale in the surrounding area. The long-range transport towards Pic Du Midi site pointed out also potential contributions connected to the exchange between the marine environments and the atmosphere and to possible dust events from North Africa.

1. Introduction

The research dedicated to studying the atmospheric transport of microplastics has been advancing in recent years. Microplastics are defined as fragments, fibres and films of plastic with dimensions in the range from 1 μm to 5 mm. Their release in the environment is connected uniquely to anthropogenic activities, by domestic, industrial and agricultural sources. Processes such as the abrasion of daily-life plastic objects, including clothes, recycling or incineration of plastic wastes, traffic emissions by tyres and brakes, plastic mulching, sewage sludge used as fertiliser, degradation of plastic used for greenhouses, contribute to the microplastic population in the environment (see e.g. Mbachu et al., 2020; Shao et al., 2022). However, an accurate quantification of the actual emissions from these sources is a research issue that still needs to be unfolded.

Microplastics have been found in urban sites (Dris et al., 2015; Klein and Fischer, 2019; Wright et al., 2020; Truong et al., 2021), in Oceans (Liu et al., 2019; Allen et al., 2020; Trainic et al., 2020; Wang et al., 2020; Allen et al., 2022), and remote areas like mountainous sites, the Arctic and Antarctic (Bergmann et al., 2019; Allen et al., 2019; Zhang et al., 2021; Allen et al., 2021; Aves et al., 2022; Bergmann et al., 2022), indicating the role of regional and long-range dispersion in the atmosphere. Brahney et al. (2021) suggest that "*Akin to global biogeochemical cycles, plastics now spiral around the globe with distinct atmospheric, oceanic, cryospheric, and terrestrial residence times*", highlighting the importance of studying the plastic cycle and the contribution of the atmospheric transport in it.

A fundamental aspect governing the scale of the motion of airborne tracers in the atmosphere is the daily development of the boundary layer and the possible exchange of mass with the free atmosphere above it. Clearly, whenever pollutants enter the free atmosphere, they may be transported for longer distances due to stronger winds, suppressed turbulent diffusion and reduced removal processes, referring to gravitational settling and dry deposition. Microplastics are released in the air inside the planetary boundary layer, where main sources are located. Their long-distance transport is thus strongly related to how effectively particles can enter the free atmosphere and be moved far from the release area. A few contributions studied this aspect, with different approaches.

Gonzalez-Pleiter et al. (2021) investigated the occurrence, spatial distribution, shape, and chemical composition of microplastics sampled above the planetary boundary layer, by aircraft flying up to ~ 3500 m over different urban and rural areas in Spain. Numerical simulations were performed using HYSPLIT model (HYbrid Single-Particle Lagrangian Integrated Trajectory, Stein et al., 2015) to evaluate the atmospheric transport and deposition of microplastics. They provided a first evidence of microplastic presence in the free atmosphere, discussing the potential long-range transport of particles released in the sampling areas.

Such evidence was shown also by the results of Allen et al. (2021), who studied the pathways of plastic particles detected in the air at the remote and high-altitude site Pic du Midi in the French Pyrenees, using both HYSPLIT and FLEXPART (FLEXible PARTicle dispersion model, Pisso et al., 2019) Lagrangian models, identifying the locations of potential source areas. The hypothesis at the basis of their study is that finding microplastics in the free atmosphere would imply that the microplastic pollution, generated in the lower atmosphere, has the potential to influence remote and isolated areas. They considered that the top-mountain site is only occasionally affected by the pollution transported by thermal winds from the air masses in the valley boundary layer. We notice that sampling at the top of the mountain still means sampling inside the local atmospheric boundary layer, given that a boundary layer develops anywhere above the surface, as a consequence of the radiative processes and wind shear. Even if the Pic Du Midi samples may not be strictly representative of free-atmosphere air masses, indeed given that no local sources are on site, the microplastics sampled there can be interpreted as evidence of long-range transport, since the upslope and valley transport is said to be effective only occasionally.

A quantitative estimation of the microplastic concentration at the global scale was carried out by Evangeliou et al. (2022). Through the extrapolation of regional emissions and inverse modelling, they calculated global emissions of microplastics and reproduced their dispersion at the global scale. They considered that microplastic concentrations decline substantially from the surface, where microplastics are emitted, to higher altitude in the planetary boundary layer or in the free troposphere, providing an evaluation of the relative percentage of decrease.

In this research context, atmospheric dispersion models have been increasingly applied, in backward mode to trace back the provenience areas of microplastics and in forward mode to assess the impact of known emissions at the local up to the global scale (Allen et al., 2019; Evangeliou et al., 2020; Allen et al., 2021; Gonzalez-Pleiter et al., 2021; Brahney et al., 2021; Evangeliou et al., 2022). In particular, Lagrangian dispersion models of different degrees of complexity, have been applied in this field. They are based on a frame of reference moving with the average atmospheric motion and range from a simple procedure, generating deterministic trajectories, to more advanced approaches, reproducing the dispersion of airborne pollutants through the turbulent motion of fictitious numerical particles. The mean component and turbulent diffusion of the particle movement are respectively determined by the local wind velocity and its fluctuations, these last being solutions of Lagrangian stochastic differential equations.

In a former contribution (Martina and Trini Castelli, 2023), we investigated the potential role of the long-range transport applying the Lagrangian particle dispersion model MILORD (Model for the Investigation of Long Range Dispersion, Anfossi et al., 1995) to the case study discussed by Allen et al. (2019), the first work addressing the transport of microplastics detected at a remote mountain catchment in the French Pyrenees. The long-range transport was found to be more feasible for microplastics characterised by a low settling velocity, and to be more reliably related to tracer parcels travelling in the free atmosphere and reaching the receptor site after entrainment from it into the atmospheric boundary layer. Here we extend our analysis of the long-range transport in the troposphere by investigating the effectiveness of the exchange between the planetary boundary layer and the free atmosphere. We refer to the case studies of Gonzalez-Pleiter et al. (2021) and Allen et al. (2021), above introduced, since they gave the first evidence of the presence of microplastics in the free atmosphere. In the first case, we aim at tracing the potential source areas of the microplastics detected in the free atmosphere and

Table 1
Gonzalez-Pleiter et al. (2021) case study. Details of the three flights of the experimental campaign: the sampling took place in the morning, from 9 am to 1 pm Local Time (UTC+2)

Flights	Date	**cities covered**	**characteristics**
Flight 1	April 25, 2018	Madrid–Tarancón	rural areas
Flight 2	May 23, 2019	Alcalá de Henares, Guadalajara, Valladolid	rural and suburban areas
Flight 3	June 17, 2019	Madrid, Guadalajara	highly populated areas

at discerning whether the microplastics released in a city, like Madrid, may feasibly represent the main source for their presence in the free atmosphere above it, or whether the long-range transport may be more effective, conversely. In the second case, we investigate whether the microplastics reaching a remote mountain-top are mostly conveyed there by travelling in the free atmosphere, compared to the transport in the boundary layer. The relative effectiveness of the long-range transport and of the vertical dispersion between the boundary layer and the free atmosphere is considered. A comparison with the findings in Allen et al. (2021) work, where two different Lagrangian models were used, also enables assessing the feasibility and reliability of MILORD model in reproducing the MP dispersion in the atmosphere even in its relatively simple configuration.

Microplastic(s), Planetary Boundary Layer and Free Atmosphere in the following are also referred to with the acronyms 'MP(s)', 'PBL' and 'FA', respectively. The two case studies and related results are summarised in Section 2, in Section 3 the main characteristics of the MILORD model are recalled and the performed simulations are presented. The main results achieved through various model simulations are discussed in Section 4 and conclusions are given in Section 5.

2. The case studies

For our investigation, we chose the two case studies by Gonzalez-Pleiter et al. (2021) and Allen et al. (2021) because they were the first original works addressing the presence and transport of MPs in the FA, and posing the question of how ubiquitous such an emerging pollutant is in the atmosphere. Quantifying the intrusion of MPs from the PBL into the FA enables not only determining the potential global scale of their transport, but is also a first step to establishing whether a 'background concentration' of MPs in the air is already recognisable.

In both works numerical models were used, allowing us also to evaluate the applicability of our long-range dispersion model MILORD, by comparing the results of our backward and forward simulations with their original outputs and findings.

In the following sub-sections, a description of the two case studies and a summary of the results achieved by Gonzalez-Pleiter et al. (2021) and Allen et al. (2021) are reported.

2.1. Synopsis of the experimental campaign and numerical simulations by Gonzalez-Pleiter et al. (2021)

Gonzalez-Pleiter et al. (2021) is the first and among the few works reporting experimental evidence of the presence of MPs above the PBL. An experimental campaign was carried out by sampling MP concentration in the air through three aircraft flights, from an altitude of $\simeq$ 700 m up to $\simeq$ 3500 m a.s.l., over both high and low-populated areas in central Spain, near the city of Madrid and in the suburban and rural surroundings, south-east, north-east and north-west of the city. In Table 1 the main details of the flight campaign are reported. The authors considered that most of the MPs were sampled above the PBL, given that in the area its typical heights range from 500 m to about 2000 m a.s.l.. Air samples were collected with filters, their microparticle content (both natural and anthropic) was analysed and MPs were identified. The highest MP concentration was found above Central Madrid, while the values were decreasing in less populated urban areas and rural regions.

Numerical simulations forward in time were then performed using the HYSPLIT model, driven by the GDAS (Global Data Assimilation System) meteorological data, to evaluate the atmospheric transport and deposition of the sampled MPs. A unitary 1-hour release from the region of Central Madrid, in correspondence to coordinates 40.4167°N latitude and 3.70325°W longitude, was reproduced on June 17 2019, starting at 0900 a.m. local time (UTC+2), assuming that MPs were homogeneously distributed. The MP mass was released in the FA at the median sampling altitude over Madrid, 2800 m a.s.l., and the simulations lasted 1 h, 12 h, 24 h and 36 h. The emitted mass ($1.1676\ 10^{12}$ MPs) was calculated based on the MP average concentration (13.9 ± 8.7 MPs/m^3) measured in the sampling area (84 km^2).

The MP deposition was shown to occur mostly close to the source area, and a secondary deposition trace was found near the Biscay Bay (see Fig. 4 in Gonzalez-Pleiter et al., 2021). The presence of MPs in northern France indicated that MPs may travel long distances away from their initial source. Based on their analysis, Gonzalez-Pleiter et al. (2021) concluded that densely populated cities can be an important source of MPs in the atmospheric compartment. Thus urban areas could be sources of MPs that may then be transported and deposited at distant areas, shedding light on the role of long-range atmospheric dispersion.

2.2. Synopsis of the experimental campaign and numerical simulations by Allen et al. (2021)

The experimental campaign carried out by Allen et al. (2021) revealed the presence of MPs in the air, at the meteorological station of Pic Du Midi, located in the French Pyrenees (42° 56′ 11″ N, 0° 8′ 3″ E, 2877 m a.s.l.). The observational period covered four months, from June 23 to October 23 2017, and from active aerosol samplings MP particles were counted to estimate their relative concentration. Each sampling period lasted 7 days, each day from 21 to 14 UTC next day, for a total of 15 analysed samples characterised by about 70% of fragments and 30% of fibres, the latter identified as the particles with a length-to-width ratio of 3:1.

Several numerical 7-days-long simulations were performed, using both the HYSPLIT model, to trace the back trajectories and obtain air–mass particle history trajectories, and the FLEXPART model, taking into account the mixing between the PBL and the FA and the atmospheric turbulence, to identify the potential source regions. For HYSPLIT a back-trajectory was run for each hour during the sampling period, starting at an altitude of 100 m a.g.l. (~3000 m a.s.l.) and using ECMWF (European Centre for Medium Range Weather Forecasts) ERA-Interim analyses as meteorological input. In FLEXPART, for each hour of the sampling period, a continuous backward release of particles was done, at the site altitude of ~ 3000 m a.s.l.. The 3-hourly meteorological ECMWF ERA-Interim analyses, with a grid resolution of 0.5° × 0.5°, were used as input.

Simulations showed that on average, the traced-backward air masses maintained an elevation above 2000 m a.s.l., travelling a minimum of 275 km from the sample site over the full period. The authors noticed that for periods when the sampled MP quantities were large, the atmospheric transport occurred at lower elevations than for periods with fewer sampled MPs. Simulations related to samples with a higher amount of measured MPs showed a majority of trajectories crossing the Mediterranean Sea and Northern Africa. The trajectories connected to the lower amount of sampled MPs were instead arriving from

the Atlantic Ocean and North America. The authors found a positive correlation between the number of trajectories falling inside the mixing zone between the PBL and the FA and the average number of MPs arriving at the site. Such correlation was found both for the ocean and land areas, implying that land might not be necessarily a greater MP source influence and that MPs transported over the ocean into the FA through mixing might be both of terrestrial or marine origin. Based on the model simulations, they concluded that MPs may travel in the FA and that trans-ocean and trans-continental MP transport, thus long-range may occur, highlighting also the role that PBL plays in determining the MP concentration in the air masses, depending on their size.

3. The MILORD model simulations

MILORD is a stochastic Lagrangian particle dispersion model and was conceived to be a numerical research tool to simulate and predict on long-range the transport, dispersion, removal and deposition of tracers from accidental releases (Anfossi et al., 1995; Desiato et al., 1998; Trini Castelli, 2012). The model was applied to study the impact of releases of radioactive substances after the Chernobyl accident (Anfossi et al., 1995) and from the Fukushima nuclear power plant (Boetti et al., 2018). MILORD was validated based on model intercomparisons in these contexts, achieving excellent results. The model was used also in the backward mode, to identify the potential source areas leading to peaks of CO_2 and Black Carbon concentrations observed at the background station of Plateau Rosa mountain observatory, 3480 m a.s.l in the Italian Alps (Ferrarese and Trini Castelli, 2019; Ferrarese et al., 2024). Its first application to study the atmospheric dispersion of microplastics is documented in Martina and Trini Castelli (2023), and some additional investigation can be found in Martina et al. (2022, 2025). Details of the equations, parameterisations and algorithms implemented in MILORD can be found in the above cited articles.

Here we recall that the topography and meteorological input are derived by the ECMWF analysis fields. MILORD is a Random Displacement Model, calculating the stochastic Langevin equation for the displacement of emitted virtual particles, representing a mass of the tracer or pollutant. The atmospheric dispersion is determined by a deterministic term, given by the advection due to the wind, and a stochastic term related to the turbulent diffusion. Short-time or continuous releases from point, line or area sources are treated, simulating the particle dispersion over scales from regional to long-range, from hundreds to thousand kilometres in space, and from one day to months in time. It is important here to remind that the development of the PBL follows a daily cycle and its height is calculated each time step at the specific location corresponding to the particle position. The method for calculating the PBL height is relatively simple and reproduces a growth of the convective layer during the day, accounting for the local dawn and sunset times and for the value of a mixing length representative of the mechanical turbulence, this last characterising even the stable conditions during night and the reduced PBL depths over the sea. The vertical motion of the Lagrangian particle is determined by the vertical component of the wind velocity and the vertical diffusivity. The only condition allowing the Lagrangian particle to cross the PBL height during its motion, and to move between the PBL and the FA, depends on the variation of the PBL height along its trajectory. A particle may pass from the PBL to the FA or viceversa only if, during the integration timestep, the PBL height becomes respectively lower or higher than the height at which the particle is moving. Despite the simplicity of the approach, analogous distributions of the particle trajectories inside and above the PBL were found when comparing MILORD simulations to those using FLEXPART model driven by a regional meteorological model in complex terrain (Ferrarese and Trini Castelli, 2019; Ferrarese et al., 2024).

Dry and wet deposition, and when needed radioactive decay, contribute to the depletion of the mass particle during its atmospheric motion, based on exponential reduction equations. All particles moving within the so called 'precipitation layer' (typically up to a height of 5000 m in MILORD) contribute to the wet deposition, while only the particles travelling inside the PBL contribute to the dry deposition. When MILORD is used in the backward mode, a particle moving back in time inside the PBL can re-gain the corresponding mass that would be depleted in the forward motion, at each timestep.

In the following subsections, the configuration of MILORD model for the simulations of the two case studies is illustrated. The meteorological input files were elaborated by the ECMWF analyses, acquiring the fields on both a 0.5° × 0.5° grid, the grid resolution originally and typically used by MILORD model, and a 0.25° × 0.25° grid, to have the option of resolving the topography and atmospheric circulation in a more detailed way. An algorithm based on successive iterations, computing temporary displacements subject to a convergence condition (Reap, 1972), enables assigning physically reasonable positions to the pollutant particle when dealing with coarse-gridded meteorological input fields, both in time and space. This makes MILORD able to solve the transport suitably even at shorter scales than long-range. Analyses addressing MILORD sensitivity by varying the spacing of the input gridded fields did not show notable discrepancies, even close to the source.

We focused our investigation on the atmospheric dynamics determining the motion of the air masses containing the pollutant, where the MPs are treated as passive tracers. Thus, the possible effects related to the interaction between the atmospheric motions and particles of different shapes are not considered. To distinguish among different MP sizes or types, we performed simulations using settling velocities that characterise fibres or fragments.

3.1. MILORD simulations for the case study Gonzalez-Pleiter et al. (2021)

Several simulations were performed, both in forward and backward modes, in application to the Gonzalez-Pleiter et al. (2021) case study. The main goals were to (i) investigate whether the MPs sampled in the FA originate in the Madrid area or whether they might be transported there by regional or long-range distances, (ii) to assess the proportion of air parcels, containing the MPs, that are travelling into the PBL or in the FA, and (iii) to evaluate the time and spatial scales of the impact of Madrid city as a source of MPs.

The numerical domain considered for the simulations covered an area from 30°W to 50°E in longitude and from 35°N to 75°N in latitude. The emission source is centred in Madrid coordinates (40° 30′N, 3° 40′W) and at different heights depending on the specific run. Here we show results for simulations using in input the ECMWF meteorological fields over a 0.25° × 0.25° grid, and a time step $\Delta t = 1080$ s. The number of Lagrangian particles released for each simulations was $N_L = 10^3$, each representing an ensemble of $m_i = \frac{Q_{tot}}{N_L}$ MPs, where $Q_{tot} = 10^{12}$ MPs is the number of MPs estimated by Gonzalez-Pleiter et al. (2021) within the considered emission volume. This last was determined on the area of 84 km^2 and a height of 1 km or 10 m depending on where the release is performed, in the FA or when considering the city as an area source inside the PBL. Table 2 summarises the specific sets of parameters used for the different simulations, introduced in the following.

- **Run_F_FA**. Forward simulations, emission in the free atmosphere.

This simulation was aimed at replicating the simulations in Gonzalez-Pleiter et al. (2021), in order to verify that MILORD results are in agreement with theirs. A single release lasting 1-Δt was reproduced and the particles were followed for 7-days, from June 17, 2019 at 07:00 UTC to June 24, 2019 at 07:00 UTC. The first 36 h covered the time period considered in Gonzalez-Pleiter et al. (2021), the following days

Table 2
Main details of the MILORD model configuration for the Gonzalez-Pleiter et al. (2021) case study. The simulation period is 1 week for all runs.

Parameter	Run_F_FA	Run_F_PBL	Run_F_PBL_24h	Run_B_FA
Type	Forward in FA	Forward in PBL	Forward in PBL	Backward in FA
Spatial resolution (degree)	$0.25° \times 0.25°$	$0.25° \times 0.25°$	$0.25° \times 0.25°$	$0.25° \times 0.25°$
Time step Δt (s)	1080	1080	1080	1080
Release height a.s.l. (m)	2300–3300	677–687	677–687	2300–3300
Release duration	1 Δt	1 Δt	24 h	1 Δt
Settling velocity v_s (ms^{-1})	0.1	variable	0.1	0.1

Table 3
Values of the settling velocity estimated for airborne MPs in literature.

Reference	Settling velocity (ms^{-1})	Particle types	Dimensions (μm)
Allen et al. (2019)	0.1	dust particles	25
Wright et al. (2020)	0.32	non-fibrous microplastics, spherical	100
	0.06	fibrous microplastics	diameter/length = 20/400
Trainic et al. (2020)	0.001	sub-micron particles	< 1

Table 4
Main details of Allen et al. (2021) samples selected for the simulations and of the MILORD model configuration.

Sample Code	Measured $\overline{N_{MPs}}/m^3$ (mean ± std)	period of sampling and of (backward) simulation	number of particles	period of release
A02	0.66 ± 0.04	04 - 11/07/2017		
A07	0.09 ± 0.02	16 - 22/08/2017	1000 each Δt	21 – 14 UTC each day
A14	0.34 ± 0.04	10 - 17/10/2017		

were examined to investigate the potential impact areas on a longer time scale.

The source volume was centred at the median altitude of 2800 m, as reported in Gonzalez-Pleiter et al. (2021) for their simulation on the same day, June 17 at 07:00 UTC, and the particle were released in the FA at heights ranging from 2300 to 3300 m.

- **Run_F_PBL**. Forward simulations, emission within the boundary layer: Madrid as a source.

The goal of these simulations was to test the hypothesis of Madrid as an active source of MP pollution above its own PBL and in the surrounding areas. To this purpose, the 1-Δt particle emission, simulated in Run_F_FA, is reproduced in **Run_F_PBL** with a release within Madrid PBL, to investigate the scale of the particle dispersion. In this context, we evaluated the effect of different MP settling velocities, v_s, on the area of impact. We considered four values, as reported in Table 3, chosen from related literature following Allen et al. (2019), Trainic et al. (2020) and Wright et al. (2020), who estimated the settling velocity based on different theoretical approaches. Low values of v_s generally refer to fibres while higher values are more representative for fragments.

A second simulation, **Run_F_PBL_24h**, reproduced a one-day continuous release inside the PBL, and aimed to investigate the potential role of the entrainment of particles in the FA above the source accounting for the different stability conditions that develop during the day, from stable to convective. The emission was started on June 16 at 00:00 UTC and continued along all day, the simulations lasted one week, until June 23 at 00:00 UTC.

For both runs, the emission volume had its base 15 m above Madrid's altitude and a thickness of 10 m, so that particles were emitted at heights ranging from 677 to 687 m a.s.l., to be representative of an urban area source.

- **Run_B_FA**. Backward emission in the free atmosphere.

In this simulation, the trajectories of the Lagrangian particles that arrived in the sampling volume were traced backward. The goal was to identify the provenience areas and possible sources of the MPs detected in the FA above Madrid, to investigate the potential efficacy of the long-range transport more in depth. The emission date, the simulation period and the backward-release volume, here treated as receptor, were the same as simulation **Run_F_FA** but backward trajectories were reconstructed. Specific parameters are reported in Table 2.

3.2. MILORD simulations for the case study Allen et al. (2021)

In application to the case study of Allen et al. (2021), three simulations were performed, covering three different sampling periods. The selection was done considering samples having respectively a high (code A02), an average (code A14) and a low (code A07) concentration of measured MPs with respect to the average observed during the entire campaign. In Table 4 the main characteristics of the chosen samples are reported.

To trace the provenience areas, the back trajectories of the Lagrangian particles were recreated considering a continuous back-release lasting for the sampling hours 21–14 UTC of every single day in the sampling period, and the simulations, referred as **Run_B_A##**, lasted 7 days. The volume of the backward source, corresponding to a receptor, was defined with a horizontal extension of 20×20 m and a vertical extension of 100 m and was centred at Pic Du Midi coordinates (42° 56′ 11″ N, 0° 8′ 34″ E), at a height of ~ 3000 m a.s.l. (~100 m a.g.l.), as done by Allen et al. (2021). The simulation domain extends from 20°N to 80°N and 30°W to 30°E. The ECMWF analyses on a $0.5° \times 0.5°$ resolution grid were used in input, using the same grid spacing as in Allen et al. (2021), and the timestep was set to $\Delta t = 2160$ s.

The identification of the MP provenience areas accomplished with MILORD simulations is firstly verified by comparing them with Allen et al. (2021) results. Then, the main goal here is to further investigate the respective roles of the local, regional and long-range transport, addressing whether the MPs reach mountainous remote sites mostly travelling in the FA and which is the potential contribution of the dispersion in the PBL.

3.3. Elaboration and analysis of the simulation outputs

To analyse the results, the simulation outputs were processed in different ways. Plots of the trajectories and their relative frequency inside the PBL or in the FA were produced, for both forward and backward runs. Contour maps of deposition and concentration fields were elaborated for the forward runs. The computational grid on which these quantities were processed had a resolution of about $0.1° \times 0.1°$ in longitude and latitude. We recall that only the particles travelling inside

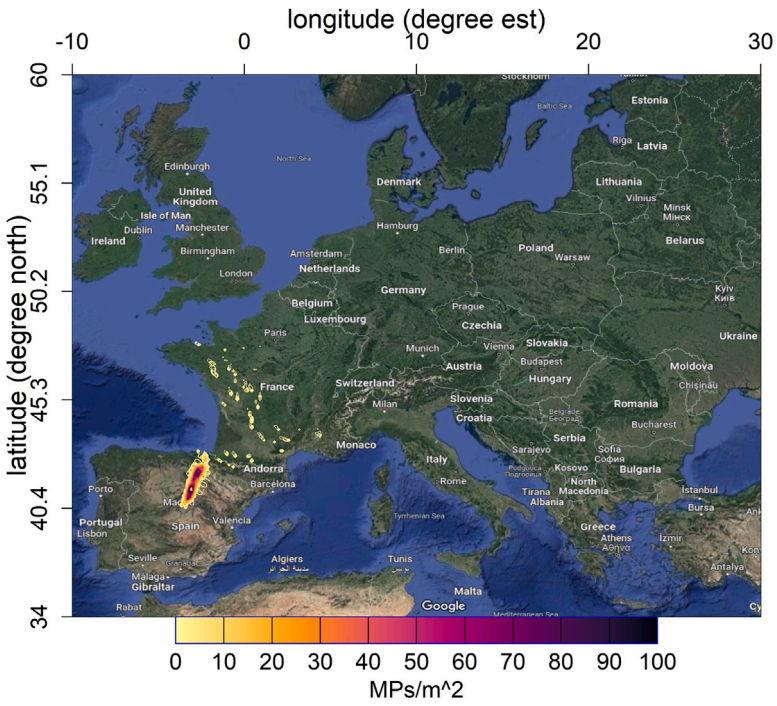

Fig. 1. Run_F_FA. Contour of the MP cumulated deposition field (MP number/m^2) after 36 h of simulation, referred to Fig. 4 in Gonzalez-Pleiter et al. (2021). Map by Google©.

the PBL contribute with their pollutant mass to the dry deposition at the ground and to the concentration in the air. For the backward runs polar plots of the relative frequency of trajectories taking place in the PBL or in the FA were prepared, by counting the particles passing through the single cell in the post-processing grid.

To investigate the potential entrainment inside the PBL of particles released in the FA, the heights at which they are travelling were considered, the percentage of particles travelling above the PBL to the total number of active particles is plotted as a function of time, where with 'active' it is intended the particles in the troposphere that are still inside the simulation domain at a given time.

In addition, their mass was considered to estimate the relative percentage of particles travelling inside or above the PBL, and to assess the reliability of the predicted distance the particles may have travelled before reaching the site, referring to the back trajectories. We recall that in MILORD the tracer mass in the Lagrangian particle may decrease by deposition in forward mode or increase when back-trajectories are re-constructed, by re-gaining what would be deposited in a corresponding forward run. Let us define N_p the number of Lagrangian particles for which $M(t_{end}) \leq \Gamma M(t_{beg})$, where $M(t_{beg})$ and $M(t_{end})$ are the masses at the beginning and at the end of the particle trajectory, respectively, and Γ represents the corresponding ratio of mass increase during the backward travel. Considering only the contribution of dry deposition and defining $\beta = \frac{N_p}{N_{tot}}$, where N_{tot} is the total number of released particles, we can estimate the percentage of particles that do not change their mass, thus travelling in the FA and having $\Gamma = 1$, and those that re-gain their mass, thus travelling inside the PBL and having $\Gamma > 1$. The plausibility of the travel distance may thus be inferred by considering a realistic mass increase.

4. Results of MILORD numerical simulations and discussion

The main results derived from the various numerical simulations are discussed, mainly considering (i) the distances from a city source at which MPs can be dispersed, also depending on the effect of their settling velocity, and (ii) the potential distances travelled by MPs before arriving at a remote receptor site and the efficacy of the long-range transport inside the PBL and in the FA.

4.1. Results for Gonzalez-Pleiter et al. (2021) case study

The **Run_F_FA** simulation reproduced the MP dispersion after their release in the free atmosphere above Madrid as done in Gonzalez-Pleiter et al. (2021), to compare MILORD simulation outputs with their results.

Fig. 1 shows the deposition pattern 36 h after the emission. Two main areas of cumulated deposition, calculated as number of MPs in a m^2, are identified. The main one extends about 350 km north-east of Madrid, generated during the first 24 h. Then sparse zones are tracked in the central-northwest side of France, originated by masses arriving there from 24 up to 36 h after the release and passing over the Biscay Bay. To compare the dispersion pattern obtained by MILORD simulations with the results of Gonzalez-Pleiter et al. (2021), as in their Figure 4, the locations of the puff of particles are depicted in Figure 1 of the Supplementary Material, at 1, 12, 24 and 36 h after the release. The results of the numerical simulations with MILORD are overall comparable with those obtained with the HYSPLIT model, both qualitatively and quantitatively.

Fig. 2a shows the percentage of the Lagrangian particles travelling inside the FA (blue line) over the total number of active particles (green line). The number of particles moving above the PBL is mostly close to the total number of active particles, except for some periods of entrainment into the PBL related to its daily cycle. This remarks that particles released in the FA tend to stay in the FA. This analysis confirms the deposition pattern in Fig. 1, showing that the major contribution to deposition occurred within the first 36 h, when the number of particles travelling within the PBL is larger. Notice that the number of Lagrangian particles decreases in time because they start exiting the simulation domain, becoming inactive.

To determine the potential contribution of Madrid city as a source of MPs in the FA above its area, we refer to the results of **Run_F_PBL**, considering the emission within the PBL. Firstly we determined the extension of the areas around the source that are affected by the MP deposition at the ground, looking also at the corresponding MP concentration in the air. In this context, we tested the sensitivity to the settling velocity values, for both fragments and fibres (Table 3), by comparing their MP deposition and concentration fields in the domain.

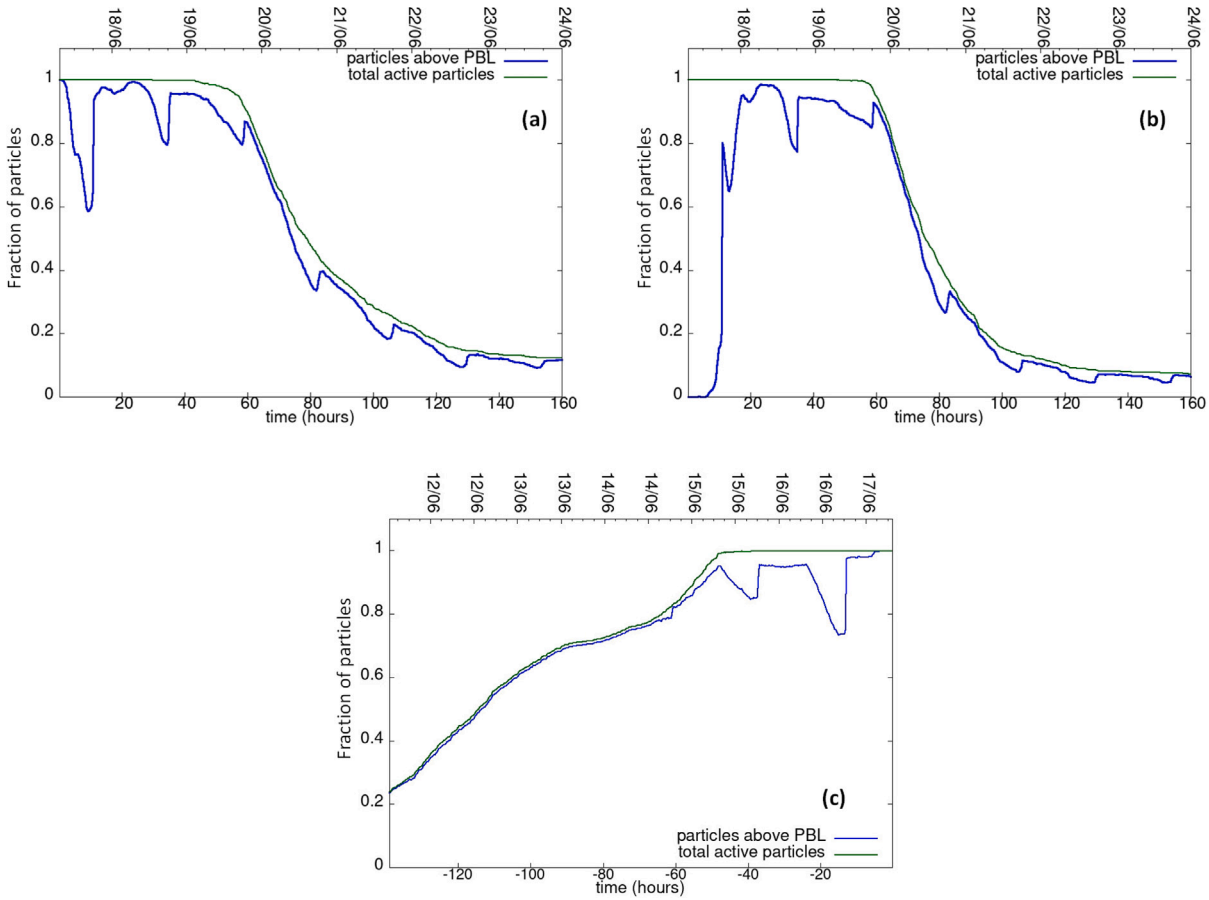

Fig. 2. Fraction of particles travelling above the PBL (blue line) as function of time, for the $1-\Delta t$ release simulations Run_F_FA (a), Run_F_PBL (b) and Run_B_FA (c). The green line indicates the number of active particles in percentage with respect to the total released particles.

Fig. 3 reports the contour plots representing the patterns of concentration (left column) and deposition (right column) for the four different settling velocities. As expected, for larger values of v_s higher levels of deposition are found closer to the source, whereas for the lowest v_s the particles maintain a larger mass thus leading to higher air concentrations over longer distances from the release location. To assess the effect of the alternative settling velocities, here representing different types of MPs, we normalised the values of the deposition and concentration obtained with $v_s = 0.001, 0.06, 0.32$ ms^{-1} to those using $v_s = 0.1$ ms^{-1}, adopted for the other simulations. In Figure 2 of the Supplementary Material the curves of the normalised quantities are plotted as a function of the distance from the source. The variable behaviour of the curves depicting the ratios depends on the relative efficacy of the deposition and on the tracer content that remains in the Lagrangian particle and can still undergo deposition while moving further from the source. Within a 100 km distance, the ratios for the deposition (concentration) vary as $0.02-0.45$, $0.76-2.8$ and $1.31-7\times10^{-4}$ ($2.54-47$, $1.4-4.7$, $0.35-2\times10^{-4}$) for $v_s = 0.001, 0.06, 0.32$ ms^{-1}, respectively. This provides an estimate of the order of magnitude of the variability that can be expected when characterising the MPs through their settling velocity. It confirms, also through a quantitative comparison, that fibres and sub-micron plastic fragments are more likely subjected to long-range transport, given that they are associated with lower values of the settling velocities.

To address the potential transport in the FA of the MPs emitted from Madrid inside the PBL, we tracked the height at which the particles are travelling. Fig. 2b highlights that, after their release in the PBL, the particles tend to move remaining inside it for a relatively long time period (~10 hours, see also Figure 3 in the Supplementary Material) before starting to enter the FA. Therefore their passage from the PBL over the urban area to the FA above it, in the experimental period and conditions considered, does not appear to be efficient.

To further assess the efficiency of Madrid as a potential active source of MP pollution above its own PBL, we refer to **Run_F_PBL_24h** where a 24-hours continuous emission was simulated and followed for 1 week, using $v_s = 0.1$ ms^{-1}. During the simulation, about 10^{-3} of the released particles moved into the FA above Madrid's area considering a $\simeq 25$ km radial extension. To determine the potential distance covered by the particles released in the PBL, then travelling in it or moving into the FA, in Fig. 4 the distributions of their positions during the simulation period are plotted. Overall, the particles enter the FA at a distance of about 150–200 km from the source, then keep mostly travelling in it. These findings suggest that the emission from the city may not significantly contribute to the pollution in the FA above its own PBL. In the distribution, we notice a peak in the number of particles at about 300 km distance. This may be related to the plume impinging on the mountainous Pyrenees arc. The increase of the number of particles inside the PBL at distances between 750 and 950 km reflects the deposition traces found in **Run_F_PBL** in the north-western of France.

Fig. 5 shows the percentage of particles travelling in the FA compared to the total number of active particles. During the first 20 h of continuous release only a fraction of particles move into the FA (~20% maximum after about 10 h), and just after such period most of the particles are entrained within the FA. In the following hours, the cyclic variation of the number of particles travelling inside the FA is connected to the daily cycle of the PBL, that is the growth of a convective boundary layer, when thus particles may be captured back inside it by the entrainment process.

Also considering a continuous emission, thus itself subjected to a variable and time-dependent interaction with the atmospheric processes, the exchanges of masses between the PBL and the FA above

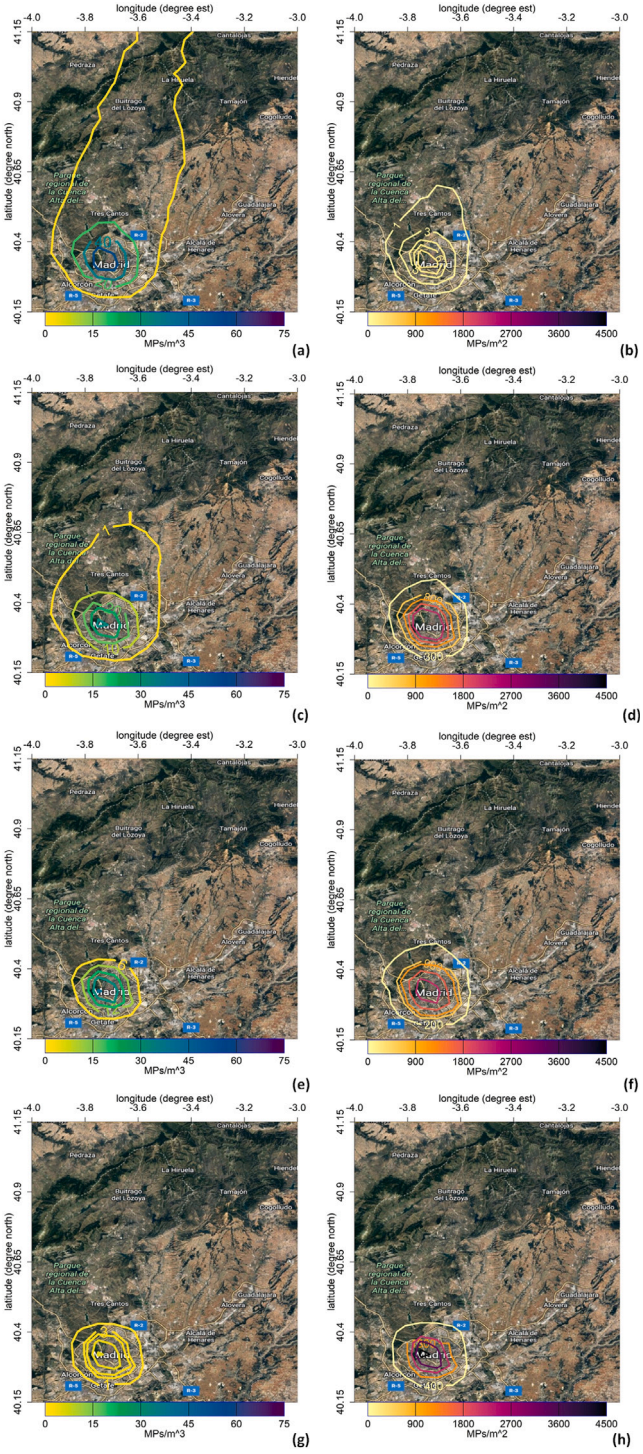

Fig. 3. Run_F_PBL. Contours of the concentration (a,c,e,g) and deposition (b,d,f,h) fields for different settling velocities: 0.001 ms^{-1} (a,b), 0.06 ms^{-1} (c,d), 0.1 ms^{-1} (e,f), 0.32 ms^{-1} (g,h).

it appear to be not efficient in the vicinity of the release source. This indicates that the contribution from Madrid might not necessarily be the primary one for the MPs detected in the FA above its area, and that those MPs might have originated in other areas, then being transported there by regional or even longer-range distances.

Whether the higher number of MPs detected above Madrid's area compared to the rural areas was related to the MP emission from the city itself, as reasonably hypothesised by Gonzalez-Pleiter et al. (2021), cannot be decisively and finally determined, because the samplings were carried out in different periods. This implies that different meteorological conditions could have been the driver of different MP concentrations, beyond the role played by the emission sources. Thus it would not be possible to disentangle the two contributions, release and transport, in a conclusive way.

Through the backward simulation performed in **Run_B_FA** it was then possible to identify the potential areas of provenience of the MPs detected in the FA above the Madrid area. Besides tracking the particles' back trajectories, we analysed how realistic their travel distance could be. Fig. 6 reports the distribution of the back-trajectories frequency, for the particles travelling in the FA (top panel) and in the PBL (bottom panel), through contour plots in percentage. The most frequent trajectories of Lagrangian particles that travelled in the FA come from the south-west, with a second signal from the north. The frequency of particles moving into the PBL is much lower, they come from the south-west and from shorter distances, as expected. The trajectory patterns of all particles and of those travelling above the PBL are reported in Figure 4 of the Supplementary material.

In Table 5 the different values of the β parameter computed after one and two days of simulation – when the total number of active particles starts to decrease because they exit the simulation domain – are reported for $\Gamma = 1$ and for three ranges of its value, considering an increase of the particle mass from 1.5 to 10 times the original value. This can give an indication of the time and space scales of the particle travels, also connected to the reliability of having an initial mass more and more loaded with MPs. As reported in the Table, most of the particles keep their mass unchanged ($\Gamma = 1$), which implies that they have travelled in the FA where settling processes are not effective. This remarks that particles that arrived at the quote reported by Gonzalez-Pleiter et al. (2021) tend to have travelled within the FA, thus to have originated at larger distances than local ones.

The percentages of particles that increased their mass, for $\Gamma \neq 1$, are related to masses moving inside the PBL. The value of the percentage gives a hint of the time the particles spent in the PBL, a period during which they earned back their MP content in the backward modality of the MILORD model. In one day the particles that increase their mass by more than 5 times are a bit more than 19% and then almost 26% after two days, when the percentage of particles with a mass ten times larger than its final value increases much. This Γ value may be retained as a reasonable threshold, suggesting that possible MP sources laying inside the PBL are to be searched within the first days of simulation, thus at distances characteristic of a local or regional scale.

These findings are confirmed by looking at Fig. 2c. Before entering the sampling area in the FA, part of the Lagrangian particles (10–20%) moved inside the PBL within the previous couple of days, but not in the time frame immediately before they arrived at the receptor point. Notice that in the days before reaching the receptor area, the particles were mostly travelling over the Ocean, where the PBL height is low and kept constant. Thus the exchange of mass between the PBL and the FA is not efficient and the active particles tend to remain in the FA layer where they entered.

4.2. Results for Allen et al. (2021) case study

The runs **Run_B_A##** simulated a continuous backward emission of particles during the three selected periods out of the samplings presented and discussed in Allen et al. (2021) study. This enables to identify the potential source areas of the MPs detected at the high altitude of Pic Du Midi station and to address the spatial scale of their travel before reaching the site.

Fig. 7 shows the contour plots of the trajectory frequencies for the sample A02 (top), A07 (centre) and A14 (bottom). The contours produced separately for the trajectories of particles travelling in the FA and inside the PBL are reported respectively in Figures 5 and 6 of the Supplementary Material. The outputs of MILORD are in agreement with

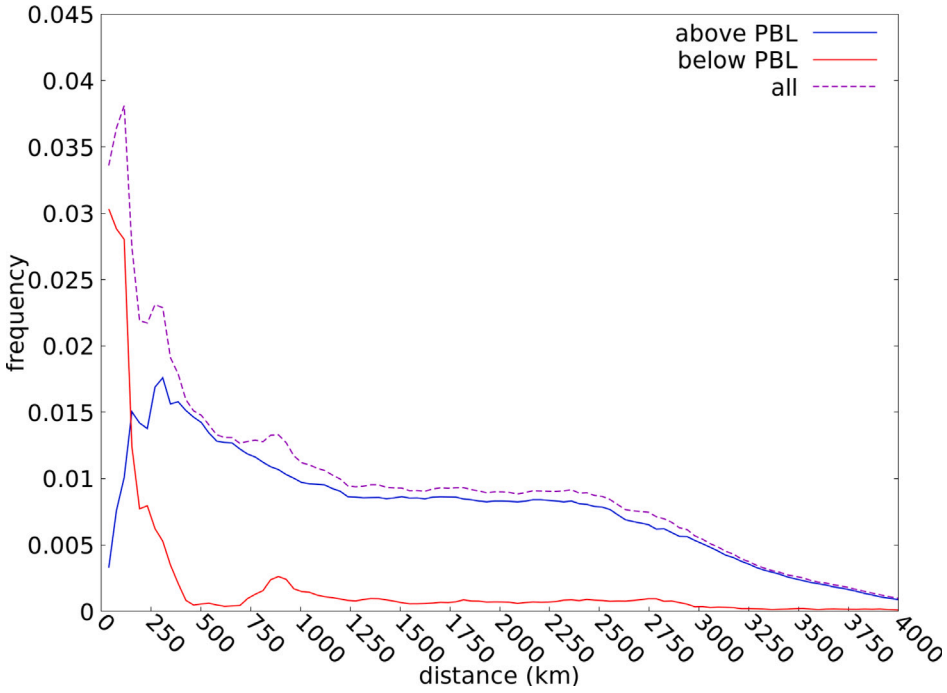

Fig. 4. Run_F_PBL_24 h distance distribution for simulated particles. The red line refers to particles travelling within the PBL while the blue line refers to particles travelling within the FA. The dashed violet line refers to the total number of particles.

Table 5
Run_B_FA. Percentage of particles expressed by the β parameter for different Γ intervals, after a simulation period of 1 and 2 days.

Index	β (1st day)	β (2nd day)
$\Gamma = 1$	72.1%	65.4%
$1 < \Gamma < 1.5$	0.4%	0.8%
$1.5 < \Gamma < 5$	8.1%	7.9%
$5 < \Gamma < 10$	4.5%	4.4%
$\Gamma > 10$	14.9%	21.4%

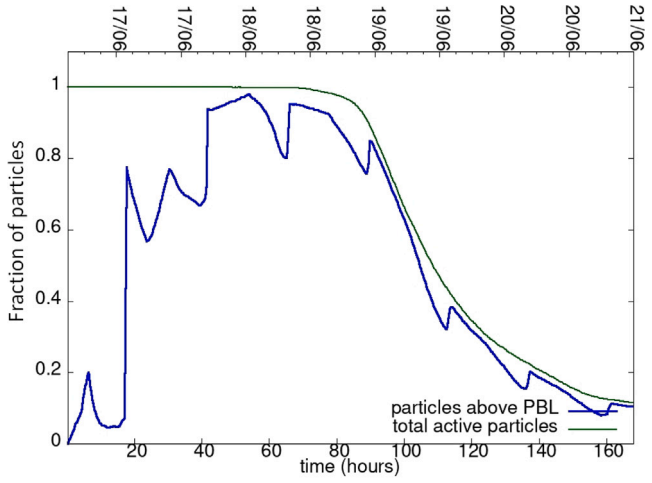

Fig. 5. Run_F_PBL_24 h. Fraction of particles travelling above the PBL (blue) and the total number of active particle (green) as a function of time.

the results of Allen et al. (2021), as reported in their Supplementary Material, Figure 2 and Figure 3. The provenience areas of the air masses for case A02 are in the highest percentage from south-south-west, then from north-west and south-east. A clear signal from North Africa connected to the highest amount of detected MPs is caught in **Run_B_A02**. The provenience areas in **Run_B_A07** are from west-north-west, crossing the Atlantic Ocean before arriving at the site. In **Run_B_A14** the direction of provenience is west-south-west and south-east, brushing the north-west coast of Africa.

To compare our simulation results with the findings in Allen et al. (2021), in Table 6 we report the values of some of the quantities given in their work and that we were able to estimate, considering that the single Lagrangian particle in MILORD is not tagged. Given the differences in the Lagrangian models and the approach used, and considering that they are applied on long-range, such comparison has to be interpreted as indicative of trends more than of absolute values. Here $\langle z \rangle$ is the average height a.s.l. at which the particles travel during the simulation period, calculated by averaging the particles' heights at each time step and then applying an average over the full simulation periods; $\langle d \rangle$ is the average distance covered by the particles and was calculated as the average of the distances reached by the particles from the release point at the last time step; d_{max} is the maximum distance reached by an active particle. The average quote $\langle z \rangle$ is generally higher than in Allen et al. (2021). As additional information, in Figure 7 of the Supplementary material the time evolution of the average height is plotted together with the percentiles of its distribution. The average quote in MILORD keeps being above 3000 m in all cases, with some difference in the vertical spreading of the backward plume reaching the receptor point. Particles travelling close to the ground start lifting towards the site about 25 h before arrival. The average distance $\langle d \rangle$ is longer in MILORD for samples A02 and A14, while shorter for A07, while the maximum distance is shorter for A02 and A07, and longer for A14, but the differences may depend also on the dimension of the simulation domain. MILORD simulations confirmed that the number of

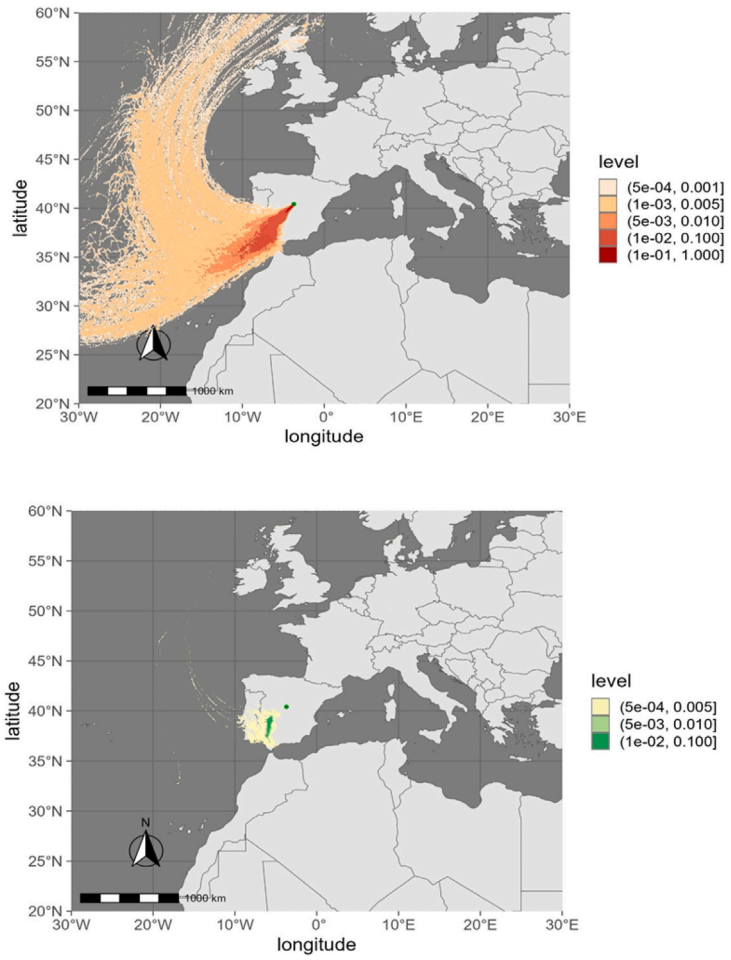

Fig. 6. Run_B_FA. Contour plot of the trajectory frequency for particles above (top) and inside (bottom) the PBL. "Level" indicates the frequency of the trajectories normalised over their total number, respectively above and within the PBL.

Table 6
Run_A##. Estimates of the parameters characterising the backward dispersion for the three cases, compared to the Allen et al. (2021) ones.

Cases	$< z >$ (m a.s.l.)	$< d >$ (km)	d_{max} (km)	N_{PBL} (%)
A02 (MILORD)	3663	3272	4221	8.
A02 (Allen)	2159	2047	6109	17.6
A07 (MILORD)	3563	3412	4193	5.1
A07 (Allen)	3022	4895	7890	0.3
A14 (MILORD)	3767	3281	3669	5.6
A14 (Allen)	3188	2721	1328	3.1
$N\_MP > 0.33$ (Allen)	2747 ± 373	4992 ± 1097		9. ± 6.
$N\_MP < 0.33$ (Allen)	3276 ± 425	3332		2. ± 1.

particles travelling inside the PBL is found to be greater for the case of the highest number of MPs in the sample, as for A02 one.

To distinguish the potential source areas of particles travelling in the FA or inside the PBL, then arriving at Pic Du Midi site, we refer to the polar plots in Figs. 8 and 9, representing the respective frequency in percentage of the trajectories in the domain. The percentage is calculated normalising respectively to the total number of trajectories above the PBL and inside it. The centre of the plot is positioned at Pic Du Midi coordinates and the distribution of the frequency of trajectories is shown up to 1500 km distance from the receptor site.

Besides identifying the areas of provenience separated depending on the travel quote, the polar plots better highlight the distances characterising the regions of greater contribution, which generally stay within less than 500 km. The signal from North Africa is clearly linked to the long-range transport in the FA, as seen in Run_B_A02. The pathways over the Ocean are also mostly associated with the transport in the FA, looking at Run_B_A07 and Run_B_A14 in Fig. 8. As for the plots of frequency inside the PBL (Fig. 9), it is interesting to notice the occurrence of signals also at distances farther than 1000 km, from south-south-east and some traces from the west for Run_B_A02, from north-west and just a light trace from east-south-east in Run_B_A07, from west-south-west and weaker from south-east in Run_B_A14. Such signals cover both land and marine environments, the Atlantic Ocean and the Mediterranean Sea. The trajectories inside the PBL covering marine areas indicate that part of the MPs reaching the Pic Du Midi site may have originated from the exchange and fluxes between the sea and the atmosphere, as it happens for sea salt and aerosol. The presence of such signals also above the PBL may be related to the exchange of air masses between the PBL and the FA, which can be effective during their long-range motion. Of course, the efficacy of such exchange depends on how the PBL daily variation is modelled, in a rather simplified way in MILORD.

In Fig. 10 the percentage of particles travelling above the PBL, normalised to the total number of active particles, is reported during

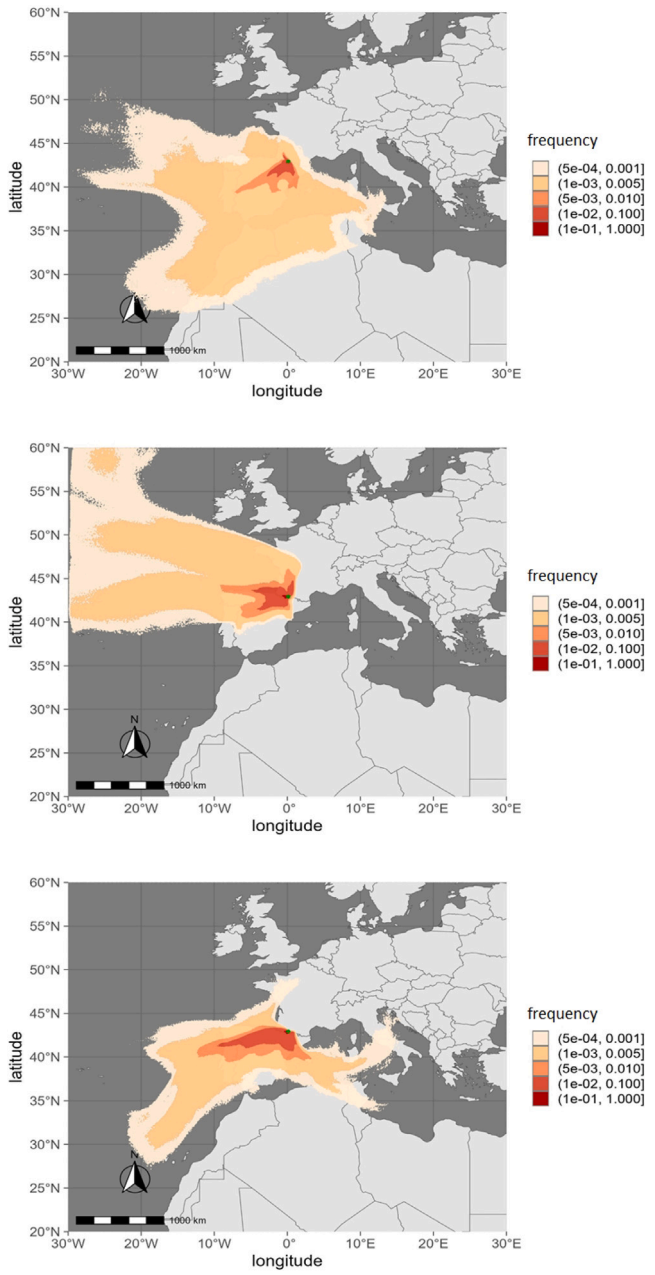

Fig. 7. Contour of the percentage of the trajectories for the A02 case (top), A07 (centre) and A14 (bottom).

the sampling periods for the three simulations. It highlights that the largest part of the trajectories take place in the FA, confirming the role of long-range transport. The effect of the PBL daily cycle is also evident, more marked for the summer periods, leading to an increase of tracer masses entraining in it from the FA. To provide a quantification, the values of the Γ parameter were calculated also for the three 7-day periods of this case study, as reported in Table 7. It was found that the percentage of Lagrangian particles maintaining their mass along all the simulation period ($\Gamma = 1$), thus always travelling in the FA, is larger for the samples containing the lowest number of MPs, as A07 case, while it is confirmed that the majority of the particles travel inside the PBL for the sample with the highest number of MPs, A02. An intermediate distribution of the percentages is found for the average MP concentration related to A14 sample. The majority of the particles that have been travelling in backward mode inside the PBL ($\Gamma \neq 1$) earned back less than 5 times their initial MP content, about 49% for A02, 23% for A07 and 31% for A14 over the total number of particles. The threshold $\Gamma < 5$ also in this case can be retained as a reasonable reference to infer the time and space scales of the transport from potential MP sources inside the PBL. Comparing the Γ values with the correspondent in Table 5 for Gonzalez-Pleiter et al. (2021), where the MPs were collected fully in the FA and the mass transport occurred mostly in it, it may be inferred that the MPs samples collected in Allen et al. (2021) may be more reasonably representative of air parcels moving at the boundary between the PBL and the FA, as discussed in the introduction. We estimated that the average time spent by a particle in the PBL was, for both case studies, of the order of one day.

5. Summary and conclusions

In this work, we investigated the role of the long-range atmospheric transport in determining the presence of microplastics collected in the free atmosphere and at a high mountain top, where the contribution from the local transport due to the up-valley thermal winds might be assumed to be poorly effective. Even if we do not consider the air sampling at a mountain-top as made directly in the free atmosphere, given the remote and high altitude conditions the presence of microplastics can be retained as evidence of long-range transport.

We referred to two previous studies, respectively Gonzalez-Pleiter et al. (2021) addressing the presence of microplastics in the free atmosphere above the Madrid region, and Allen et al. (2021), investigating the origin of microplastics collected in the air at Pic du Midi monitoring station. Simulations with the Lagrangian particle dispersion model MILORD were conducted, both in forward and backward modes. Firstly, we verified that the MILORD simulations were correctly reproducing the dispersion patterns presented in the two studies. Backward simulations enabled us to determine the time and space scales of the transport inside and above the atmospheric boundary layer, and to identify the possible source regions and related microplastic pathways. Our investigation highlighted the predominant role of long-range transport in both cases. It was possible to estimate that the time scale related to the transport inside the boundary layer is of the order of one to a few days, for distances from tens to a few hundred km.

In application to Gonzalez-Pleiter et al. (2021) case, the motion of the microplastics detected in the free atmosphere above Madrid was followed in forward mode for the following couple of days, showing that most particles that entered the free atmosphere tend to remain inside it for some hundred km before passing into the boundary layer where they contribute to ground deposition. In addition, we investigated whether the city of Madrid may be considered an effective source of microplastics in the free atmosphere above its area and which could be instead source regions of particles from long distances. The simulations showed that the tracer emitted from the city tends to disperse over distances of tens to a few hundred km, before entering the free atmosphere. Advection can be expected to play a major role in transporting air masses containing a pollutant released close to the ground or, anyway, inside the boundary layer. We thus retain that a city like Madrid may weakly contribute as a direct microplastic source for the free atmosphere above its area, probably only in strong convective conditions when the entrainment process between the atmospheric boundary layer and the free atmosphere can be more effective. This aspect needs additional deepening, by using Lagrangian models that solve the atmospheric processes at the regional and local scale, thus able to reproduce the exchanges between the boundary layer and the free atmosphere with a more advanced and refined approach. Using a long-range model with a relatively simple parametrisation of the boundary-layer daily development, like MILORD, may limit the accuracy of the results. However, the strength of the Lagrangian models, being themselves grid-free, is that the parcel motion is followed at all scales with the same accuracy, leading to a complete description of all the phases of dispersion, close and far from the source. Thus, the predictions provided by MILORD simulations can be considered

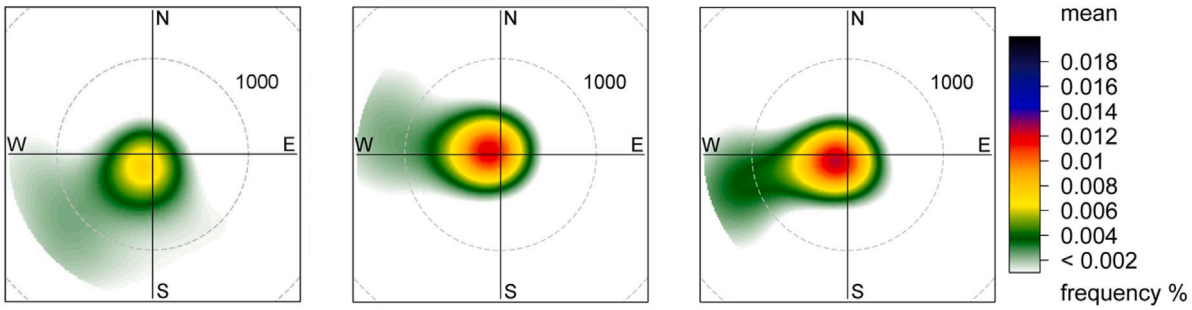

Fig. 8. Polar plot of the frequency of the particle trajectories above the PBL for Run_B_A02 (left), Run_B_A07 (centre) and Run_B_A14 (right). The percentage is calculated normalising to the total number of trajectories above the PBL.

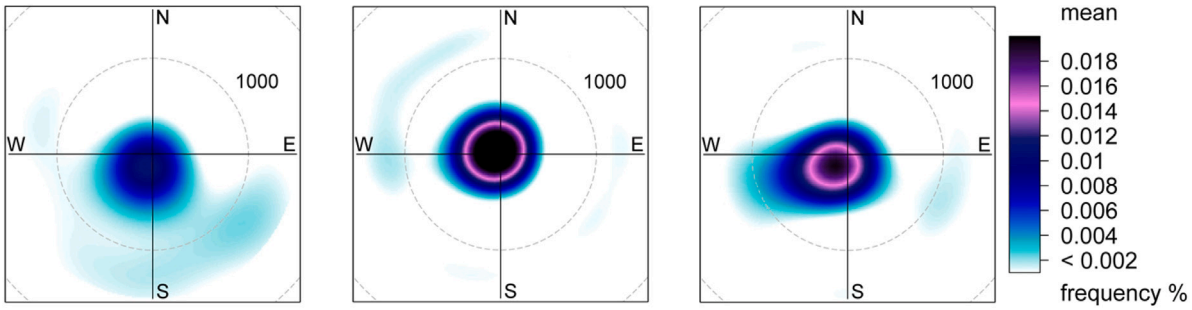

Fig. 9. Polar plot of the frequency of the particle trajectories inside the PBL for Run_B_A02 (left), Run_B_A07 (centre) and Run_B_A14 (right). The percentage is calculated normalising to the total number of trajectories inside the PBL.

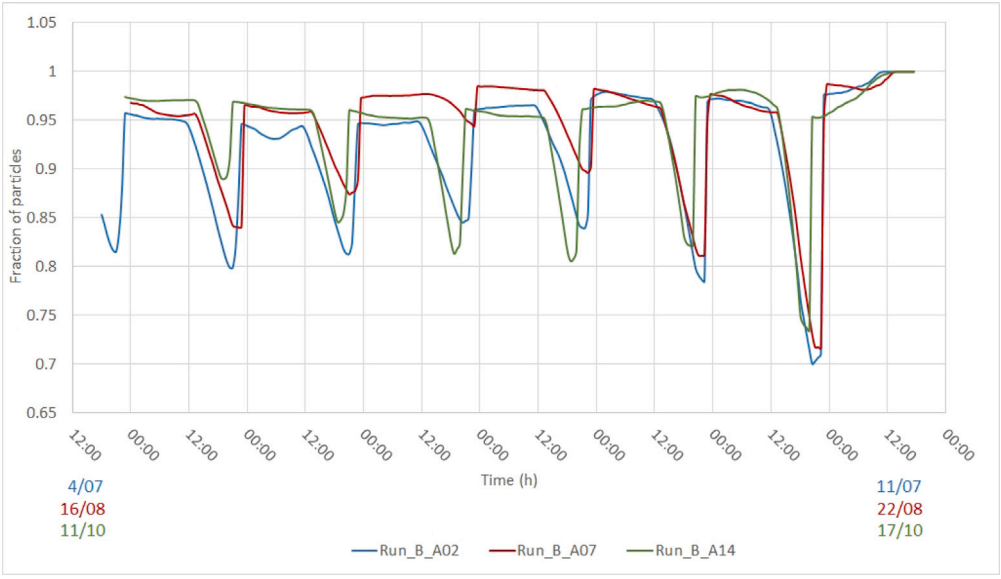

Fig. 10. Fraction of particles above PBL normalised to the number of active Lagrangian particles, for Run_B_A02 (blue line), Run_B_A07 (red line) and Run_B_A14 (green line).

Table 7
Runs_A##. Percentage of particles expressed by the β parameter for different Γ intervals, after a simulation period of 7 days.

Index	β A02	β A07	β A14
$\Gamma = 1$	36.2%	71.9%	61.3%
$1 < \Gamma < 1.5$	28.2%	16.1%	20.4%
$1.5 < \Gamma < 5$	21,%	7.1%	10.2%
$5 < \Gamma < 10$	5.2%	2.6%	3.3%
$\Gamma > 10$	9.4%	2.3%	4.8%

sufficiently reliable in depicting the dispersion trend even at scales finer than long-range.

For the Allen et al. (2021) case study, we traced back the potential source areas in three different periods, related to high, low and average numbers of sampled microplastics. It was found that even if most particles moving inside the boundary layer were travelling over land, a signal was found of particles arriving at the site after passing over the Atlantic Ocean or the Mediterranean Sea. This result gives an indication of the potential role of the marine environment as a source of microplastics, which can enter the atmosphere and be transported over long distances. The contribution of oceans and seas to microplastics in the atmosphere was suggested and discussed in Allen et al. (2020), Evangeliou et al. (2020), Allen et al. (2021), and the possible mechanisms of the microplastic exchange between the sea and the air were investigated by Shaw et al. (2023). Yet, the share of the marine environment to the atmospheric microplastic budget is still an open issue (Yang et al., 2022; Brahney et al., 2021) and needs further studies. The MILORD simulations also confirmed the pathways originated from North Africa, highlighting the potential transport of microplastics during the dust events at the long-range scale. As in the original work, it was found that for the sample with the highest microplastic content the largest number of particles arrived at the site after travelling mostly inside the planetary boundary layer, confirming that such high concentration may occur when the mixing between the boundary layer and the free atmosphere is effective. Overall, MILORD results are in agreement with those obtained by the combination of two Lagrangian models, HYSPLIT and FLEXPART, used in Allen et al. (2021) for their advanced and in-depth study on the mixing between the boundary layer and the free atmosphere. This is additional support for retaining MILORD findings reliable enough to describe and interpret the vertical exchange of polluted parcels between these two sublayers of the troposphere.

As for the regulated air pollutants, even for microplastics numerical modelling brings a fundamental contribution both in estimating the potential impact and in providing indications to design environmental policies and strategies for emission reductions. The unknown facts and uncertainties related to studying the airborne microplastics are indeed still large, and more contributions are necessary. The implications of the microplastics' shape, generally irregular and aspherical, of their size and specific aerodynamics on modelling their atmospheric dispersion remain largely unknown. Our next research efforts aim at deepening the investigation both with an experimental approach (Musso et al., 2024), to assess the interactions of such emerging pollutant with the atmospheric processes, and with a modelling approach, using local-scale Lagrangian models like SPRAY (Tinarelli et al., 2000; Trini Castelli et al., 2023) to better represent and resolve the exchanges between the ground and the atmosphere, the boundary layer and the free atmosphere.

CRediT authorship contribution statement

Matteo M. Musso: Writing – review & editing, Writing – original draft, Visualization, Validation, Software, Methodology, Investigation, Formal analysis, Data curation. **Silvia Trini Castelli:** Writing – review & editing, Writing – original draft, Visualization, Validation, Supervision, Resources, Methodology, Investigation, Conceptualization.

Declaration of competing interest

The authors declare that they have no known competing financial interests or personal relationships that could have appeared to influence the work reported in this paper.

Acknowledgments

The authors are deeply grateful to Prof. Silvia Ferrarese, doctoral supervisor of Matteo M. Musso at the Department of Physics of Turin University, for her continuous scientific support and enlightening discussions, and for her friendship.

Appendix A. Supplementary data

Supplementary material related to this article can be found online at https://doi.org/10.1016/j.atmosenv.2025.121308.

Data availability

Data will be made available on request.

References

Allen, D., Allen, S., Abbasi, S., Baker, A., Bergmann, M., Brahney, J., Butler, T., Duce, R.A., Eckhardt, S., Evangeliou, N., Jickells, T., Kanakidou, M., Kershaw, P., Laj, P., Levermore, J., Li, D., Liss, P., Liu, K., Mahowald, N., Masque, P., Materic, D., Mayes, A.G., McGinnity, P., Osvath, I., Prather, K.A., Prospero, J.M., Revell, L.E., Sander, S.G., Shim, W.J., Slade, J., Stein, A., Tarasova, O., Wright, S., 2022. Microplastics and nanoplastics in the marine-atmosphere environment. Nat. Rev. Earth Environ. 3, 393–405. http://dx.doi.org/10.1038/s43017-022-00292-x.

Allen, S., Allen, D., Baladima, F., Phoenix, V.R., Thomas, J.L., Roux, G.Le., Sonke, J.E., 2021. Evidence of free tropospheric and long-range transport of microplastic at Pic du Midi Observatory. Nat. Commun. 12. http://dx.doi.org/10.1038/s41467-021-27454-7.

Allen, S., Allen, D., Moss, K., Roux, G.Le., Phoenix, V.R., Sonke, J.E., 2020. Examination of the ocean as a source for atmospheric microplastics. PLoS One 15, http://dx.doi.org/10.1371/journal.pone.0232746.

Allen, S., Allen, D., Phoenix, V.R., Roux, G.Le., Jimenez, P.D., Simonneau, A., Binet, S., Galop, D., 2019. Atmospheric transport and deposition of microplastics in a remote mountain catchment. Nat. Geosci. 12, 339+. http://dx.doi.org/10.1038/s41561-019-0335-5.

Anfossi, D., Sacchetti, D., Trini Castelli, S., 1995. Development and sensitivity analysis of a Lagrangian particle model for long range dispersion. Environ. Softw. 10, 263–287. http://dx.doi.org/10.1016/0266-9838(95)00001-1.

Aves, A.R., Revell, L.E., Gaw, S., Ruffell, H., Schuddeboom, A., Wotherspoon, N.E., LaRue, M., McDonald, A.J., 2022. First evidence of microplastics in antarctic snow. Cryosphere 16, 2127–2145. http://dx.doi.org/10.5194/tc-16-2127-2022.

Bergmann, M., Collard, F., Fabres, J., Gabrielsen, G.W., Provencher, J.F., Rochman, C.M., van Sebille, E., Tekman, M.B., 2022. Plastic pollution in the Arctic. Nat. Rev. Earth & Environ. 3, 323–337. http://dx.doi.org/10.1038/s43017-022-00279-8.

Bergmann, M., Mützel, S., Primpke, S., Tekman, M.B., Trachsel, J., Gerdts, G., 2019. White and wonderful? microplastics prevail in snow from the alps to the arctic. Sci. Adv. 5, eaax1157.

Boetti, M., Trini Castelli, S., Ferrero, E., 2018. Reviving MILORD long-range model for simulating the dispersion of the release during Fukushima Nuclear Power Plant accident. In: Mensink, C., Kallos, G. (Eds.), Air Pollution Modeling and Its Application XXV. pp. 387–391. http://dx.doi.org/10.1007/978-3-319-57645-9_61.

Brahney, J., Mahowald, N., Prank, M., Cornwell, G., Klimont, Z., Matsui, H., Prather, K.A., 2021. Constraining the atmospheric limb of the plastic cycle. Proc. Natl. Acad. Sci. USA (118), http://dx.doi.org/10.1073/pnas.2020719118.

Desiato, F., Anfossi, D., Trini Castelli, S., Ferrero, E., Tinarelli, G., 1998. The role of wind field, mixing height and horizontal diffusivity investigated through two Lagrangian particle models. Atmos. Environ. 32, 4157–4165. http://dx.doi.org/10.1016/S1352-2310(98)00195-2.

Dris, R., Gasperi, J., Rocher, V., Saad, M., Renault, N., Tassin, B., 2015. Microplastic contamination in an urban area: a case study in greater Paris. Environ. Chem. 12, 592–599. http://dx.doi.org/10.1071/EN14167.

Evangeliou, N., Grythe, H., Klimont, Z., Heyes, C., Eckhardt, S., Lopez-Aparicio, S., Stohl, A., 2020. Atmospheric transport is a major pathway of microplastics to remote regions. Nat. Commun. 11. http://dx.doi.org/10.1038/s41467-020-17201-9.

Evangeliou, N., Tichy, O., Eckhardt, S., Zwaaftink, C.G., Brahney, J., 2022. Sources and fate of atmospheric microplastics revealed from inverse and dispersion modelling: From global emissions to deposition. J. Hazard. Mater. (432), http://dx.doi.org/10.1016/j.jhazmat.2022.128585.

Ferrarese, S., Cravero, M., Musso, M., Trini Castelli, S., 2024. Analysis and numerical modelling of black carbon and CO2 concentration peaks at a remote mountain station. In: Mensink, C., Im, U. (Eds.), Air Pollution Modeling and Its Application XXX. Springer Berlin Heidelberg, Berlin, Heidelberg, p. 6, (in press).

Ferrarese, S., Trini Castelli, S., 2019. Detection of CO2 source areas using two Lagrangian particle dispersion models, at regional scale and long range. In: Proceedings of the 19th International Conference on Harmonisation Within Atmospheric Dispersion Modelling for Regulatory Purposes, Harmo 2019. p. 5.

Gonzalez-Pleiter, M., Edo, C., Aguilera, A., Viudez-Moreiras, D., Pulido-Reyes, G., Gonzalez-Toril, E., Osuna, S., De Diego-Castilla, G., Leganes, F., Fernandez-Pinas, F., Rosal, R., 2021. Occurrence and transport of microplastics sampled within and above the planetary boundary layer. Sci. Total Environ. (761), http://dx.doi.org/10.1016/j.scitotenv.2020.143213.

Klein, M., Fischer, E.K., 2019. Microplastic abundance in atmospheric deposition within the Metropolitan area of Hamburg, Germany. Sci. Total Environ. 685, 96–103. http://dx.doi.org/10.1016/j.scitotenv.2019.05.405.

Liu, K., Wu, T., Wang, X., Song, Z., Zong, C., Wei, N., Li, D., 2019. Consistent transport of terrestrial microplastics to the ocean through atmosphere. Environ. Sci. Technol. 53, 10612–10619. http://dx.doi.org/10.1021/acs.est.9b03427.

Martina, M., Ferrarese, S., Trini Castelli, S., 2022. Simulating the dispersion of microplastics in the atmosphere towards a remote site. In: Proceedings of the 21st International Conference on Harmonisation Within Atmospheric Dispersion Modelling for Regulatory Purposes, Harmo 2022. p. 5.

Martina, M., Musso, M.M., Ferrarese, S., Trini Castelli, S., 2025. Review of the revived and revisited long-range Lagrangian particle dispersion model MILORD. In: Mensink, C., Mathur, R., Arunachalam, S. (Eds.), Air Pollution Modeling and Its Application XXIX. ITM 2023. Springer Proceedings in Complexity. Springer, Cham, http://dx.doi.org/10.1007/978-3-031-70424-6_4.

Martina, M., Trini Castelli, S., 2023. Modelling the potential long-range dispersion of atmospheric microplastics reaching a remote site. Atmos. Environ. 312, 120044. http://dx.doi.org/10.1016/j.atmosenv.2023.120044.

Mbachu, O., Jenkins, G., Pratt, C., Kaparaju, P., 2020. A new contaminant superhighway? A review of sources, measurement techniques and fate of atmospheric microplastics. Water Air Soil Pollut. 231. http://dx.doi.org/10.1007/s11270-020-4459-4.

Musso, M.M., Harms, F., Martina, M., Fischer, E.K., Leitl, B., Trini Castelli, S., 2024. Experimental investigation of the fallout dynamics of microplastic fragments in wind tunnel: The Burnia agenda. J. Hazard. Mater. Adv. 14, 100433. http://dx.doi.org/10.1016/j.hazadv.2024.100433.

Pisso, I., Sollum, E., Grythe, H., Kristiansen, I.N., Cassiani, M., Eckhardt, S., Arnold, D., Morton, D., Thompson, R.L., Zwaaftink, C.D.G., Evangeliou, N., Sodemann, H., Haimberger, L., Henne, S., Brunner, D., Burkhart, J.F., Fouilloux, A., Brioude, J., Philipp, A., Seibert, P., Stohl, A., 2019. The Lagrangian particle dispersion model FLEXPART version 10.4. Geosci. Model. Dev. 12, 4955–4997. http://dx.doi.org/10.5194/gmd-12-4955-2019.

Reap, R.M., 1972. An operational three-dimensional trajectory model. J. Appl. Meteorol. Clim. 11, 1193–1202. http://dx.doi.org/10.1175/1520-0450(1972)011<1193:AOTDTM>2.0.CO;2.

Shao, L., Li, Y., Jones, T., Santosh, M., Liu, P., Zhang, M., Xu, L., Li, W., Lu, J., Yang, C.X., Zhang, D., Feng, X., BéruBé, K., 2022. Airborne microplastics: A review of current perspectives and environmental implications. J. Clean. Prod. 347, 131048. http://dx.doi.org/10.1016/j.jclepro.2022.131048.

Shaw, D.B., Li, Q., Nunes, J.K., Deike, L., 2023. Ocean emission of microplastic. PNAS Nexus 2, pgad296. http://dx.doi.org/10.1093/pnasnexus/pgad296.

Stein, A.F., Draxler, R.R., Rolph, G.D., Stunder, B.J.B., Cohen, M.D., Ngan, F., 2015. NOAA'S HYSPLIT atmospheric transport and dispersion modeling system. Bull. Am. Meteorol. Soc. 96, 2059–2077. http://dx.doi.org/10.1175/BAMS-D-14-00110.1.

Tinarelli, G., Anfossi, D., Bider, M., Ferrero, E., Trini Castelli, S., 2000. A new high performance version of the Lagrangian particle dispersion model spray, some case studies. In: Gryning, S., Batchvarova, E. (Eds.), Air Pollution Modeling and Its Application XIII, NATO, CCMS; European Assoc Sci Air Pollut; Riso Natl Lab; Natl Inst Meteorol & Hydrol; Bulgaria Acad Sci; 3M, Representat Off. Prestige Business Ltd., pp. 499–507, 23rd NATO/CCMS International Technical Meeting on Air Pollution Modelling and Its Applications, Varna, Bulgaria, SEP 28-OCT 02 1998.

Trainic, M., Flores, J.M., Pinkas, I., Pedrotti, M.L., Lombard, F., Bourdin, G., Gorsky, G., Boss, E., Rudich, Y., Vardi, A., Koren, I., 2020. Airborne microplastic particles detected in the remote marine atmosphere. Commun. Earth & Environ. 1. http://dx.doi.org/10.1038/s43247-020-00061-y.

Trini Castelli, S., 2012. MILORD - Reload. Model for the Investigation of Long Range Dispersion. Technical Report ISAC-TO/02-2012.

Trini Castelli, S., Uboldi, F., Tinarelli, G.L., Drofa, O., Malguzzi, P., Bonasoni, P., 2023. Tracing the origin of odour nuisance from citizens' notifications with the smart modelling system. Atmos. Environ. 312, 119992. http://dx.doi.org/10.1016/j.atmosenv.2023.119992.

Truong, T.N.S., Strady, E., Kieu-Le, T.C., Tran, Q.V., Le, T.M.T., Thuong, Q.T., 2021. Microplastic in atmospheric fallouts of a developing southeast asian megacity under tropical climate. Chemosphere (272), http://dx.doi.org/10.1016/j.chemosphere.2021.129874.

Wang, X., Li, C., Liu, K., Zhu, L., Song, Z., Li, D., 2020. Atmospheric microplastic over the South China Sea and East Indian Ocean: abundance, distribution and source. J. Hazard. Mater. 389. http://dx.doi.org/10.1016/j.jhazmat.2019.121846.

Wright, S.L., Ulke, J., Font, A., Chan, K.L.A., Kelly, F.J., 2020. Atmospheric microplastic deposition in an urban environment and an evaluation of transport. Environ. Int. 136, http://dx.doi.org/10.1016/j.envint.2019.105411.

Yang, S., Zhang, T., Gan, Y., Lu, X., Chen, H., Chen, J., Yang, X., Wang, X., 2022. Constraining microplastic particle emission flux from the ocean. Environ. Sci. Technol. Lett. 9, 513–519. http://dx.doi.org/10.1021/acs.estlett.2c00214.

Zhang, Y., Gao, T., Kang, S., Allen, S., Luo, X., Allen, D., 2021. Microplastics in glaciers of the tibetan plateau: Evidence for the long-range transport of microplastics. Sci. Total Environ. 758, http://dx.doi.org/10.1016/j.scitotenv.2020.143634.